Cancer Biol Med 2026. doi: 10.20892/j.issn.2095-3941.2025.0441

ORIGINAL ARTICLE

Expansion of IL-2-independent tumor-infiltrating lymphocytes through a feeder-free process: a preclinical study for solid tumors

Ying Zhang[1], Sicheng Du[1], Rongrui Liu[2], Chuanhua Zhao[2], Juan Li[2], Sisi Ye[2], Man Zhang[3], Xingming Ma[3], Zhou He[3], Wenjia Zhuang[3], Huajun Jin[3], Jianming Xu[2]

[1]Medical School of Chinese People's Liberation Army (PLA) General Hospital, Beijing 100853, China; [2]Senior Department of Oncology, Chinese PLA General Hospital, Beijing 100853, China; [3]Shanghai Juncell Therapeutics, Shanghai 201802, China

ABSTRACT

Objective: Conventional tumor-infiltrating lymphocyte (TIL) therapy for solid tumors relies on high-dose interleukin-2 (IL-2) during expansion and post-infusion, and promotes T-cell exhaustion and toxicity. Herein, we developed a feeder-free, low-dose IL-2 TIL expansion protocol and evaluated whether hydroxychloroquine (HCQ) or programmed cell death protein 1 (PD-1) blockade might enhance therapeutic efficacy and decrease IL-2 dependence.

Methods: TILs from multiple solid tumors were expanded *ex vivo* with decreased-dose IL-2, IL-7, and IL-15 plus CD3/CD28 co-stimulation, without feeder cells. TIL products were assessed via quality control, T-cell phenotypes, and exhaustion markers. Cytotoxic activity was measured *in vitro* through interferon-gamma (IFN-γ) release and real-time cell analysis (RTCA). HCQ-induced changes in major histocompatibility complex class I (MHC-I) and programmed death-ligand 1 (PD-L1) expression were assessed in tumor cell lines, and RTCA-based cytotoxicity was evaluated using T-cell receptor–engineered T cells (TCR-T cells). The *in vivo* efficacy of HCQ and PD-1 blockade separately combined with TIL therapy was examined in a colorectal cancer patient-derived xenograft (PDX) model.

Results: The protocol consistently produced viable TILs of favorable quality across tumor types, with variable $CD8^+$ and memory T-cell profiles. Expanded TILs showed effector-to-target (E:T) ratio-dependent tumor cell killing in RTCA and secreted IFN-γ across multiple tumor types. HCQ significantly upregulated MHC-I expression *in vitro* ($P < 0.05$) without affecting PD-L1 expression or impairing TIL proliferation, and enhanced early TCR-T–mediated killing. In the PDX model, TIL plus HCQ, compared with TIL, showed less tumor growth and greater MHC-I expression, although these differences were not significant, given the small sample size. TIL plus low-dose PD-1 blockade significantly reduced tumor volume versus the control group ($P = 0.002$) and maintained higher body weights than the TIL-only and control groups.

Conclusions: The feasibility of a feeder-free, low-dose IL-2 TIL expansion system was demonstrated. PD-1 blockade significantly enhanced antitumor activity and treatment tolerability, thus supporting its promise as an alternative to high-dose IL-2. HCQ demonstrated potential immunomodulatory effects, although its *in vivo* benefit was minimal. This strategy warrants further clinical evaluation in solid tumors.

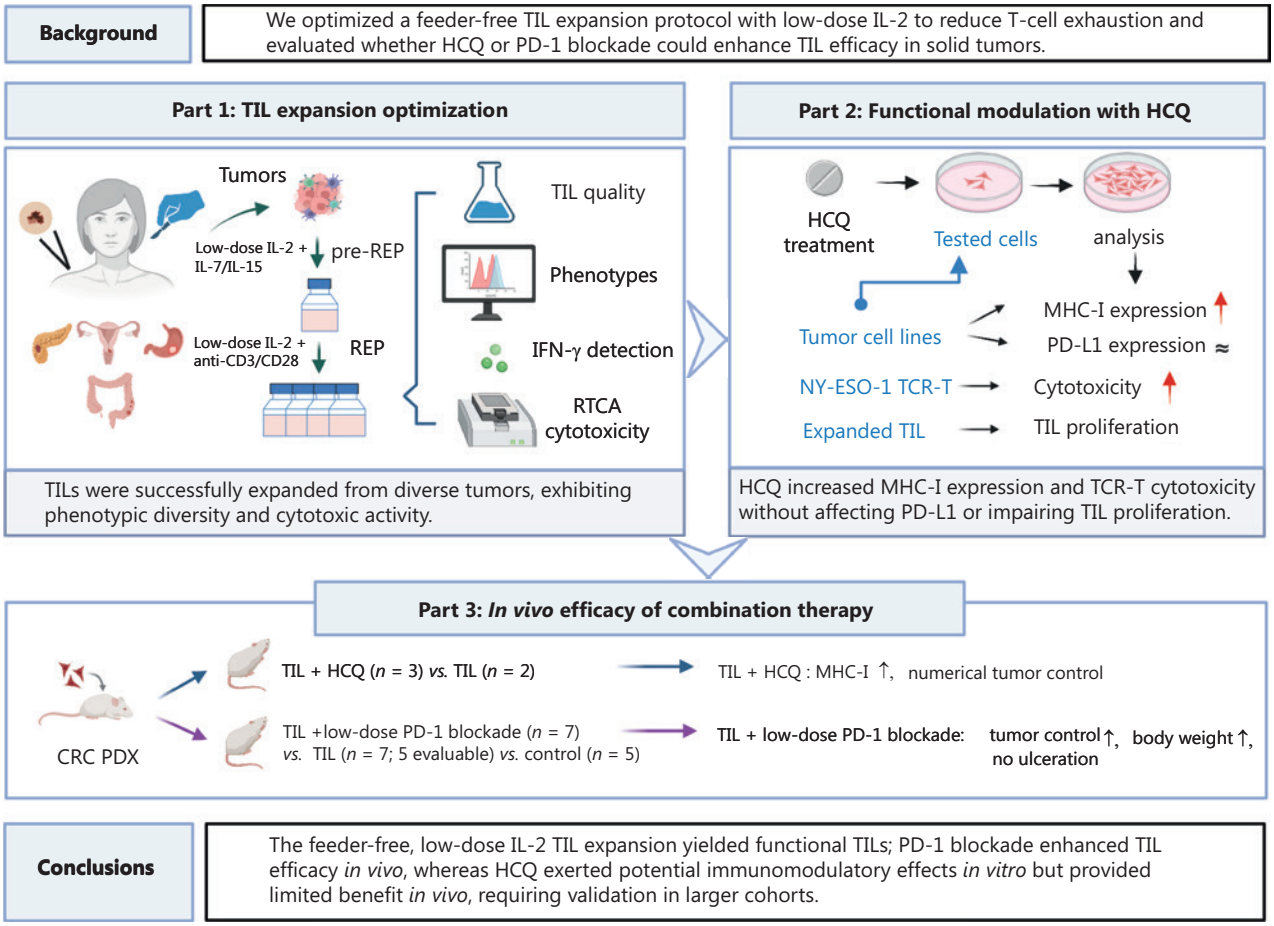
KEYWORDS Tumor-infiltrating lymphocytes; solid tumors; PD-1 blockade; hydroxychloroquine; MHC class I

Introduction

Adoptive cell therapy with tumor-infiltrating lymphocytes (TILs), a promising approach for solid tumors, uses polyclonal, tumor-reactive T cells isolated directly from tumor tissue[1,2]. Lifileucel's recent Food and Drug Administration approval for advanced melanoma supports the clinical feasibility of this strategy[3]. However, conventional TIL expansion protocols rely on high-dose interleukin-2 (IL-2) and feeder cells, which promote T-cell exhaustion and complicate manufacturing[4-6]. Lymphodepleting chemotherapy and systemic high-dose IL-2 administration further increase toxicity risks and therefore limit broader clinical use[7,8].

The young TIL approach was designed to shorten the culture duration and eliminate tumor-reactivity screening, thereby preserving less-differentiated T cells with improved *in vivo* persistence[9,10]. Nevertheless, high-dose IL-2 remains a risk factor for T-cell exhaustion[11,12]. Decreasing IL-2 levels while supplementing cells with IL-7 and IL-15 maintains

Correspondence to: Huajin Jin and Jianming Xu
E-mail: hj-jin@hotmail.com and jmxu2003@163.com
ORCID ID: https://orcid.org/0000-0002-5403-9651 and https://orcid.org/0000-0003-4467-6021
Received August 4, 2025; accepted November 4, 2025; published online March 5, 2026.
Available at www.cancerbiomed.org
© 2026 The Authors. Creative Commons Attribution-NonCommercial 4.0 International License (CC BY-NC 4.0)



Study Flow This study optimized a feeder-free, low-dose IL-2 TIL expansion system to decrease T-cell exhaustion and evaluated whether HCQ or PD-1 blockade might enhance TIL efficacy in solid tumors. Part 1: Feeder-free expansion with low-dose IL-2 plus IL-7/IL-15 in pre-REP and low-dose IL-2 plus anti-CD3/CD28 in REP consistently generated TIL products of favorable quality from multiple solid tumors, with variable phenotypes and cytotoxic activity. Part 2: *In vitro*, HCQ treatment was associated with elevated MHC-I expression on tumor cell lines and enhanced early-phase TCR-T cytotoxicity, without notable changes in PD-L1 expression or impairing TIL proliferation (as assessed by live cell counts). Part 3: In the CRC PDX model, TIL combined with HCQ (n = 3) showed a numerical increase in MHC-I expression and a numerical reduction in tumor growth, with interpretation limited by the small sample size. TIL plus low-dose PD-1 blockade (n = 7) achieved stronger tumor control, higher weight maintenance, and no ulceration, in contrast to TIL-only (n = 7 initially; evaluable n = 5 at endpoint) and control (n = 5). These findings suggested that the feeder-free, low-dose IL-2 TIL expansion yielded functional TILs. PD-1 blockade enhanced TIL efficacy *in vivo*, whereas HCQ exerted potential immunomodulatory effects *in vitro* but provided limited benefit *in vivo*. However, validation in larger cohorts is necessary. CRC, colorectal cancer; HCQ, hydroxychloroquine; IFN-γ, interferon-gamma; IL-2, interleukin-2; IL-7, interleukin-7; IL-15, interleukin-15; MHC-I, major histocompatibility complex class I; ns, not significant; PD-1, programmed cell death protein 1; PD-L1, programmed death-ligand 1; PDX, patient-derived xenograft; pre-REP, pre-rapid expansion protocol; REP, rapid expansion protocol; RTCA, real-time cell analysis; TCR-T, T-cell receptor–engineered T cell; TIL, tumor-infiltrating lymphocyte.

expansion efficiency, promotes central memory T-cell (TCM) differentiation, and decreases regulatory T-cell induction[13-15]. Additionally, CD3/CD28 co-stimulation enhances activation and decreases activation-induced cell death[16-19]. Beyond intrinsic TIL optimization, targeting tumor-intrinsic immune escape and modulating the tumor microenvironment (TME) may further improve efficacy. Major histocompatibility complex class I (MHC-I) downregulation, a key immune escape mechanism in solid tumors, impairs $CD8^+$ T-cell recognition[20,21]. Autophagy contributes to MHC-I degradation, whereas the autophagy inhibitor hydroxychloroquine (HCQ) can restore MHC-I expression and modulate antitumor immunity[22-24]. Programmed cell death protein 1 (PD-1) blockade offers an alternative to post-infusion IL-2 by reactivating exhausted T cells without associated toxicity. Notably, even low doses of high-affinity PD-1 blockade therapies, such as sintilimab, can achieve sufficient receptor occupancy for therapeutic effects[25-28].

In this preclinical study, we developed a feeder-free, cytokine-optimized TIL expansion strategy using low-dose IL-2 during *ex vivo* expansion and subsequently investigated combination approaches with HCQ or low-dose PD-1 blockade to further decrease IL-2 dependence, thereby addressing the limitations of conventional TIL therapy and informing safer, more feasible treatment options for solid tumors.

Materials and methods

TIL isolation and expansion

Tumor specimens were obtained from patients with melanoma (MM), pancreatic cancer (PC), gastric cancer (GC), cervical cancer (CxCa), or colorectal cancer (CRC). The study was approved by the Ethics Committee of the Chinese PLA General Hospital (Approval No. S2022-313-02), and informed consent was obtained from each participant before sample collection. Solid tumors were minced into small fragments and cultured in X-VIVO 15 medium supplemented with recombinant human IL-2 (2,000 IU/mL), IL-7 (10 ng/mL), and IL-15 (10 ng/mL) (all from R&D Systems) in the pre-rapid expansion protocol (pre-REP). After pre-REP culturing, TILs were transferred to the rapid expansion protocol (REP), seeded onto plates pre-coated with anti-CD3 (BioLegend) and anti-CD28 (R&D Systems), cultured for 2 days, and then transferred to G-REX100 for further expansion in REP culture medium containing X-VIVO 15 and rhIL-2 (300 IU/mL), as previously described[29,30]. The expansion success of TILs was based on the cell count; confirmation of an absence of tumor cells, mycoplasma, bacterial contamination, and tumorigenicity; and assessment of T-cell phenotypes and exhaustion markers. Cytotoxicity was evaluated through interferon-gamma (IFN-**γ**) secretion and real-time cytotoxicity assays. The final TIL products were cryopreserved in liquid nitrogen for subsequent analyses.

Quality control of expanded TILs

Cell counts were measured with acridine orange/propidium iodide (AO/PI) staining. Briefly, the cell suspensions were thoroughly mixed with 10 μL AO/PI staining solution (Countstar, cat. No. RE010212), loaded into disposable counting slides (Countstar, cat. No. C0010101), and analyzed with an automated cell counter (Countstar Rigel S2). Viable cells were identified as AO^+/PI^-. Other quality control measures included mycoplasma detection through real-time quantitative polymerase chain reaction with MycoSHENTEK DNA extraction and detection kits (cat. Nos. SK0801MY50 and SK0802MY50). Sterility testing was performed with rapid microbial methods and direct inoculation. The tumorigenicity of the final TIL products was assessed with agarose colony formation assays. All test results were confirmed to be negative.

Flow cytometry of TILs

To exclude any tumor cell contamination, we stained TILs with antibodies to CD45 (BioLegend, 304016), CD3 (BioLegend, 344804), and tumor-associated markers. Tumor cell positivity was defined as ≥ 0.01% of cells expressing any tumor marker, whereas negativity was confirmed in 3 independent replicates. For functional assessment, TILs (5×10^5 to 2×10^6 cells) were washed in DPBS and stained with fluorescent antibodies to CD45, CD3, CD4, CD8, CD45RO, and CD62L, and the immune exhaustion markers PD-1, CD39, and lymphocyte activation gene 3 (LAG-3) (all from BioLegend, cat. Nos. 304016, 344804, 317428, 344714, 304206, 304822, 367404, 328218, and 369304). After incubation for 20 min at room temperature in the dark, the cells were washed and analyzed with a CytoFLEX flow cytometer (Beckman Coulter). Data were gated on $CD45^+CD3^+$ lymphocytes. The frequency of PD-1, CD39, and LAG-3 was assessed within the $CD3^+$ T-cell population to evaluate immune exhaustion across various cancer types. Memory T-cell subsets were analyzed within the $CD4^+$ and $CD8^+$ T-cell populations. TCMs were defined as $CD45RO^+$ $CD62L^+$, whereas effector memory T-cells (TEMs) were defined as $CD45RO^+$ $CD62L^-$.

IFN-γ secretion assays

To assess cytokine secretion, we quantified IFN-γ production with an HTRF-based human IFN-γ detection kit (Cisbio, cat. No. 62HIFNGPEG). TILs were stimulated in 96-well plates pre-coated for 2 h at 37°C with anti-CD3 (Biointron, B371202), anti-CD28 (Biointron, B371201), and anti-4-1BB (Biointron, B315002-CHO) (1 μg/mL each in DPBS). The plates were washed with DPBS before use, and TILs were cultured in X-VIVO 15 medium supplemented with 5% human AB serum at 2×10^5 cells/well for 24 h. Supernatants were collected after centrifugation (1,000 × *g*, 5 min) and analyzed with a Tecan SPARK microplate reader with the HTRF module. Standard curves (0–4,000 pg/mL) were generated, and sample concentrations were interpolated with 4-parameter logistic regression. The results are expressed as pg/mL.

Real-time cell analysis

Real-time cytotoxicity assays were conducted with an xCELLigence real-time cell analysis (RTCA) DP system (Agilent Technologies) to monitor T cell-mediated tumor cell killing. Tumor cell lines were obtained from the following sources: HGC-27 from Genechem (Shanghai, China), HeLa from the Chinese Academy of Sciences Cell Bank (China), and A375 from the American Type Culture Collection. All cell lines were maintained under standard culture conditions and were routinely monitored for stable morphology. No signs of

mycoplasma contamination were observed. HGC-27 cells were seeded into E-Plate 16 plates at a density of 1×10^4 cells/well in RPMI-1640 medium containing 10% fetal bovine serum (FBS), whereas HeLa and A375 cells were seeded in DMEM containing 10% FBS. The cells were incubated overnight and cultured at 37°C under 5% CO_2. Tumor cells were incubated for approximately 24 h, after which TILs (prepared in X-VIVO 15 medium containing 5% human AB serum) or NY-ESO-1-specific TCR-T cells were added in fresh medium at the indicated effector-to-target (E:T) ratios. For TIL assays, E:T ratios of 2:1, 4:1, and 8:1 were used. In TCR-T experiments, A375 cells were pretreated with 0 or 10 μM HCQ for 48 h before co-culture, and the killing efficacy was assessed at a 1:3 E:T ratio. Tumor cell growth and cytolysis were monitored in real time according to impedance changes, which were recorded as cell index (CI) values. Decreases in CI were interpreted as a measure of tumor cell killing. The percentage of target cell killing was calculated for each well with the following formula: % killing = $[1 - (CI_t/CI_{t0})] \times 100$, where CI_{t0} is the CI at the normalization time point set approximately 5 min before effector cell addition, and CI_t is the CI at time t.

HCQ-mediated MHC-I detection in tumor cells

The human tumor cell lines A375, OVCAR-8, U-87 MG, and NCI-H2122 (all from the American Type Culture Collection) were cultured in DMEM or RPMI-1640 supplemented with 10% FBS. At 80%–90% confluence, the cells were trypsinized, seeded into 6-well plates at 3×10^5 cells/well, and cultured overnight. For drug treatment and recovery assays, cells were treated with HCQ (Shanghai Selleck, cat. No. S4430) at the specified concentrations (10 μM for A375, 15 μM for OVCAR-8 and U-87 MG, and 20 μM for NCI-H2122) for 48 h, and allowed to recover for 72 h after drug withdrawal. For programmed death-ligand 1 (PD-L1) assessment, all cell lines except OVCAR-8 were treated with vehicle (0 μM), HCQ, or recombinant human IFN-γ (3 nM; ACROBiosystems, cat. No. GMP-IFGH24) as a positive control for 48 h. The cells were then harvested and stained for flow cytometry with antibodies to HLA-ABC (BioLegend, cat. No. 311406) and PD-L1 (BioLegend, cat. No. 374514). Mean fluorescence intensity (MFI) was quantified for each marker.

Construction of NY-ESO-1-specific TCR-T cells

A codon-optimized TCR sequence (1G4-α95:LY) specific to the NY-ESO-1 peptide (SLLMWITQC) presented by *HLA-A*02:01* was synthesized (General Biosystems, China). The TCR contained chimeric human/murine constant regions to enhance correct pairing, and was flanked by EcoRI and BamHI sites for cloning. The sequence was cloned into a pHAGE lentiviral vector under control of the EF1α promoter. The sequence encoded TCRα and β chains linked by a furin-SGSG-P2A self-cleaving peptide. Lentivirus was produced in 293T cells *via* co-transfection with the psPAX2 and pMD2.G plasmids with polyethyleneimine. Human peripheral blood mononuclear cells were activated with 300 IU/mL IL-2 and 50 ng/mL anti-CD3 (OKT3) for 48 h, then transduced with concentrated lentivirus *via* spinoculation (centrifugation at 1,700 × *g* for 100 min at 32°C). Transduced TCR-T cells were expanded in X-VIVO 15 medium with 5% human AB serum and IL-2 (100 IU/mL), and TCR expression was confirmed by flow cytometry with anti-mouse TCRβ (BioLegend, cat. No. 109208) on day 7 post-transduction. The cytotoxicity of TCR-T cells against HCQ-pretreated A375 cells was assessed with RTCA experiments.

HCQ treatment and live cell counting of expanded TILs

TILs were harvested on days 10 or 11 of the REP (REP-d10 or REP-d11), resuspended, and adjusted to a final concentration of 1.5×10^6 cells/mL. The cells were seeded in 24-well plates at 1 mL/well, then treated with HCQ at final concentrations of 0 μM, 5 μM, 7.5 μM, or 10 μM, with 5 technical replicates per condition. After 48 h incubation, live cell numbers were determined with AO/PI-based automated counting.

In vivo efficacy studies in the CRC PDX model

A patient-derived xenograft (PDX) model was established by subcutaneous implantation of fragments of human CRC into 6–8-week-old female B-NDG mice (Biocytogen, China) under specific-pathogen-free conditions. The tumor implantation day was considered D0. When the tumors reached approximately 30 mm^3 (calculated as 0.5 × length × $width^2$), the mice were assigned to separate studies comparing TIL monotherapy and combination regimens. TIL therapy was administered intravenously (i.v.). For the HCQ combination study, groups (N = 5) received either TIL monotherapy (2.36×10^7 cells/mouse, i.v., once, n = 2) or TIL plus HCQ (60 mg/kg, oral gavage, administered once 1 day before TIL infusion, n = 3). The animals were euthanized on day 9 post-treatment for tumor harvesting and analysis of MHC-I expression by flow cytometry. For the PD-1 blockade study, the study groups (N = 19) received cryoprotectant vehicle control (n = 5), TIL-only (2.36×10^7 cells/mouse, i.v., once, n = 7), or TIL plus PD-1 blockade (2 mg/kg, i.v., twice weekly for the first 2 weeks and once weekly in the third week, n = 7). The study was concluded on day 21. Mice were monitored daily for general health and clinical signs. Body weight and tumor volume were recorded three times per week. Therapeutic efficacy was evaluated with complementary approaches: tumor

volume changes were monitored longitudinally to assess proliferation rates relative to the control, whereas the final antitumor activity was determined by tumor growth inhibition (TGI) based on the excised tumor weights at the study endpoint. All animal procedures were approved by the Institutional Animal Care and Use Committee of Nanchang Royo Biotech Co., Ltd. (Approval No. RYE2021102301) and were conducted in accordance with the institutional animal welfare guidelines.

Statistical analysis

All data were analyzed in GraphPad Prism 9.5.1 and SPSS 20.0. Data are presented as mean ± standard deviation (SD) or standard error of the mean (SEM). Statistical significance between two groups was assessed with unpaired *t*-tests or Mann–Whitney *U*-tests, with multiple-comparison correction when applicable. For comparisons among more than two groups, one-way or two-way ANOVA followed by Tukey's post-hoc test was applied when assumptions of normality and homogeneity were met; otherwise, the Kruskal–Wallis test followed by Dunn's post-hoc test was used. A P-value < 0.05 was considered statistically significant ($*P < 0.05$, $**P < 0.01$, $***P < 0.001$, and $****P < 0.0001$).

Results

Expansion and viability of TILs vary across tumor types during pre-REP and REP phases

TILs from MM, PC, GC, CxCa, and CRC were expanded with a two-phase protocol (**Figure 1A**), with success rates of 100.0% for MM (18/18) and GC (12/12), 92.3% for CxCa (12/13), and 90.0% for PC (9/10) and CRC (9/10) (**Figure 1B**). Only 3 cases did not expand, primarily because of small tumor specimens or low baseline TIL infiltration (**Table S1**). During the pre-REP phase (typically 10–14 days), representative TIL cultures achieved cell numbers exceeding 3×10^7 and viability generally above 80.0%. CxCa-derived TILs showed slower growth and initially lower viability, which gradually improved during this period (**Figure 1C, D**). During REP (lasting approximately 15 days), MM-derived TILs showed the highest overall expansion, approximately 2,500-fold by day 12, whereas other tumor types typically expanded less than 1,000-fold (**Figure 1E**). The daily expansion rate peaked between days 6 and 10 for most groups, and CxCa cultures showed a sharp increase (> 15-fold on day 7; **Figure 1F**). All groups showed an initial decline in viability during days 0–3, particularly CxCa, which ultimately recovered to levels > 90.0% (**Figure 1G**). All expanded TIL products passed predefined quality control criteria, including an absence of tumor cell contamination, negative sterility/mycoplasma testing, and an absence of tumorigenicity. Representative quality control data are not shown, but all samples met these thresholds and were cryopreserved for subsequent use.

Phenotypic diversity of expanded TILs across tumor types

Expanded TILs from all tumor types exhibited high purity, and that of $CD45^+CD3^+$ cells exceeded 93.0% on average and reached approximately 99.0% in MM and PC samples (**Figure 2A**). The mean proportion of $CD8^+$ T cells among $CD3^+$ cells markedly varied by tumor type, ranging from 43.6% in PC to 77.4% in CxCa (**Figure 2A**). CD39 frequency tended to be higher (approximately 68.0%) in TILs from MM, PC, and CxCa than from CRC (53.7%) and GC (45.0%). LAG-3 frequency showed moderate variability across tumor types, ranging from 37.8% in GC to 55.0% in CxCa. PD-1 levels were minimal in all groups (consistently < 0.5%; **Figure 2B**). Memory subset analysis indicated that both $CD4^+$ and $CD8^+$ TILs were dominated by TEMs ($CD4^+$: 84.7%–96.8%; $CD8^+$: 83.3%–93.9%), whereas TCMs were generally < 16.0% in all tumor types (**Figure 2C, D**). These findings indicated a consistent skewing toward an effector memory phenotype regardless of tumor origin.

In vitro antitumor cytotoxicity of TILs from various tumors

The cytotoxic activity of expanded TILs was assessed with RTCA against matched tumor cell lines: HGC-27 (GC), A375 (MM), and HeLa (CxCa). TILs induced a rapid, E:T ratio-dependent decrease in CI, and maximal cytotoxicity was observed at the highest E:T ratio (8:1). Notably, the most rapid and sustained killing was observed for HGC-27 cells, in contrast to A375 and HeLa cells (**Figure S1A–C**). An independent replicate with HGC-27 confirmed the reproducibility of these cytolytic dynamics (**Figure S1D**). Expanded TILs also secreted substantial IFN-γ levels (approximately $1.6–2.0 \times 10^4$ pg/mL) after stimulation in MM ($n = 4$), PC ($n = 3$), GC ($n = 3$), CxCa ($n = 5$), and CRC ($n = 5$) tumors, thus confirming their functional activities (**Figure S1E**).

HCQ enhances MHC-I expression and minimally affects basal PD-L1 levels in tumor cells

To investigate the immunomodulatory effects of HCQ, we treated 4 human tumor cell lines, U-87 MG (glioblastoma, $n = 4$), A375 (MM, $n = 4$), OVCAR-8 (ovarian, $n = 4$), and NCI-H2122 (non-small cell lung cancer, $n = 4$), with 10–20 μM HCQ for 48 h. Flow cytometry revealed a significant

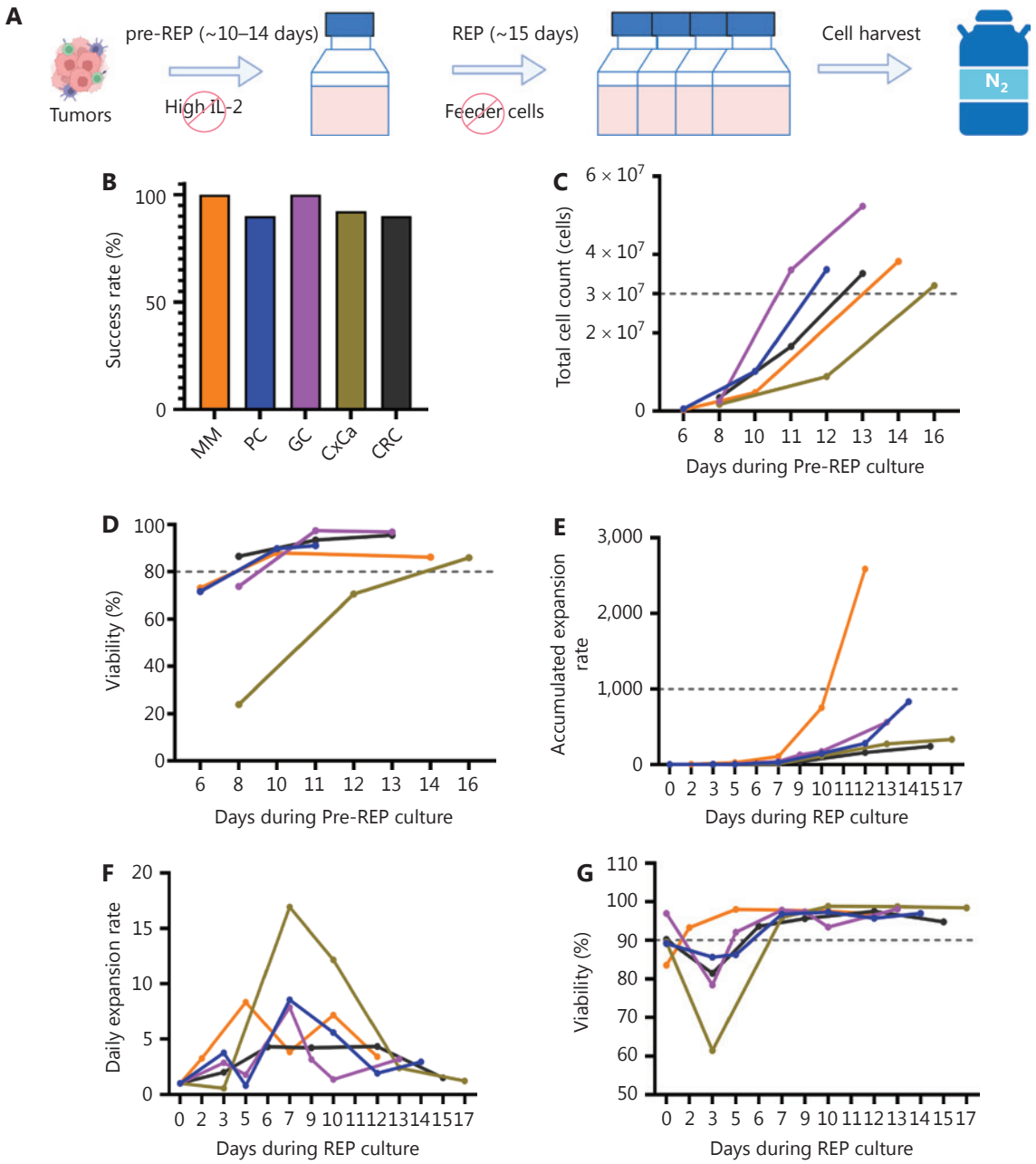


Figure 1 Expansion and viability of TILs during the pre-REP and REP. (A) Two-step expansion protocol: tumors were cultured in low-dose interleukin-2 (IL-2) during the pre-rapid expansion protocol (pre-REP) and subsequent REP without feeder cells, and harvested for cryopreservation. (B) Success rates of tumor-infiltrating lymphocyte (TIL) expansion from melanoma (MM), pancreatic cancer (PC), gastric cancer (GC), cervical cancer (CxCa), and colorectal cancer (CRC). The same color scheme is used in panels B–G to indicate tumor types. Total cell count (C) and viability (D) of representative TILs (n = 1) during pre-REP culture. Most cultures exceeded 3×10^7 cells with > 80.0% viability. Accumulated expansion rate (E) and daily expansion rates (F) during REP culture. MM showed the highest expansion (approximately 2,500-fold by day 12). (G) Viability during REP. All groups showed an early decline (days 0–3) but recovered to > 90.0%. Dashed lines indicate reference thresholds.

increase in surface MHC-I (HLA-ABC) expression across all cell lines after HCQ exposure (**Figure 3A–D**). This upregulation partially persisted after a 72-h recovery, thereby indicating a sustained effect post-treatment. We further examined whether HCQ might alter PD-L1 expression under the same conditions. The baseline PD-L1 levels were largely unaffected by HCQ treatment in all tested lines ($P > 0.05$; **Figure 3E–G**). In contrast, IFN-γ stimulation markedly upregulated PD-L1 levels ($P < 0.0001$), thus serving as a positive control and validating the assay's sensitivity.

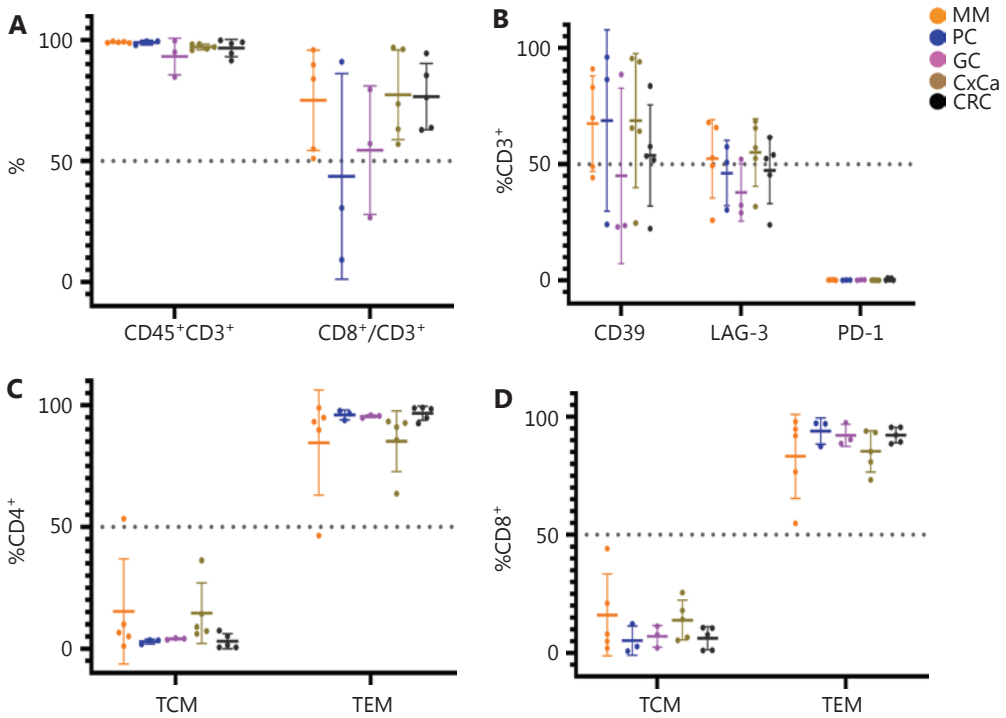


Figure 2 Phenotypic diversity of expanded TILs across tumor types. (A) Expanded tumor-infiltrating lymphocytes (TILs) showed high purity, and that of $CD45^+CD3^+$ cells consistently exceeded 93.0%. The proportion of $CD8^+$ cells among $CD3^+$ T cells varied across tumor types. (B) Frequencies of exhaustion markers within $CD3^+$ T cells: CD39 and lymphocyte activation gene 3 (LAG-3) showed variable positivity, whereas programmed cell death protein 1 (PD-1) remained negligible in all groups. (C, D) Memory subset distribution. Both $CD4^+$ (C) and $CD8^+$ (D) TILs were predominantly effector memory T-cells (TEMs), whereas central memory T-cells (TCMs) were present at low frequencies. Each dot represents one patient sample (melanoma, n = 5; pancreatic cancer, n = 3; gastric cancer, n = 3; cervical cancer, n = 5; and colorectal cancer, n = 5). Bars indicate mean ± SD. Colors represent tumor types: orange, melanoma (MM); blue, pancreatic cancer (PC); purple, gastric cancer (GC); brown, cervical cancer (CxCa); and black, colorectal cancer (CRC). Dashed lines indicate the 50% reference threshold.

HCQ enhances early-phase cytotoxicity without compromising TIL proliferation *in vitro*

To assess whether HCQ might modulate tumor sensitivity to antigen-specific cytotoxicity, we pretreated A375 MM cells with 0 μM or 10 μM HCQ for 48 h before co-culture with NY-ESO-1–specific TCR-T cells. RTCA demonstrated that HCQ pretreatment resulted in a lower baseline cell index and accelerated TCR-T–mediated killing: approximately 40.0% higher killing occurred within the first 30 h than was observed in untreated targets. This enhancement diminished over time, thus yielding an overall improvement of approximately 10.0% at the endpoint (**Figure S2A, B**). In parallel, to evaluate whether HCQ might directly influence TIL proliferation, we treated ovarian cancer–derived TILs collected at day 12 of the REP culture with increasing HCQ concentrations (0–10 μM) for 48 h. Live cell counts increased substantially over this period at all tested concentrations (**Figure S2C**). Consequently, short-term HCQ exposure did not impair TIL proliferation under these conditions.

In vivo effects of combined TIL and HCQ therapy in a CRC PDX model

Building on these *in vitro* findings, we conducted a small-scale pilot study to evaluate the combination of TIL with HCQ in a CRC PDX model. Mice receiving TIL plus HCQ (n = 3) exhibited numerically lower tumor growth metrics (**Figure S2D**) and a higher mean MHC-I expression at day 9 (**Figure S2E**) than observed in the TIL monotherapy group (n = 2). Given the extremely small sample sizes, these differences are descriptive and cannot support definitive conclusions regarding treatment efficacy. These findings are presented to inform future study design.

Efficacy and safety of TIL combined with PD-1 blockade in a CRC PDX model

In a matched CRC PDX model, mice receiving TIL plus low-dose PD-1 blockade (2 mg/kg, n = 7) maintained significantly

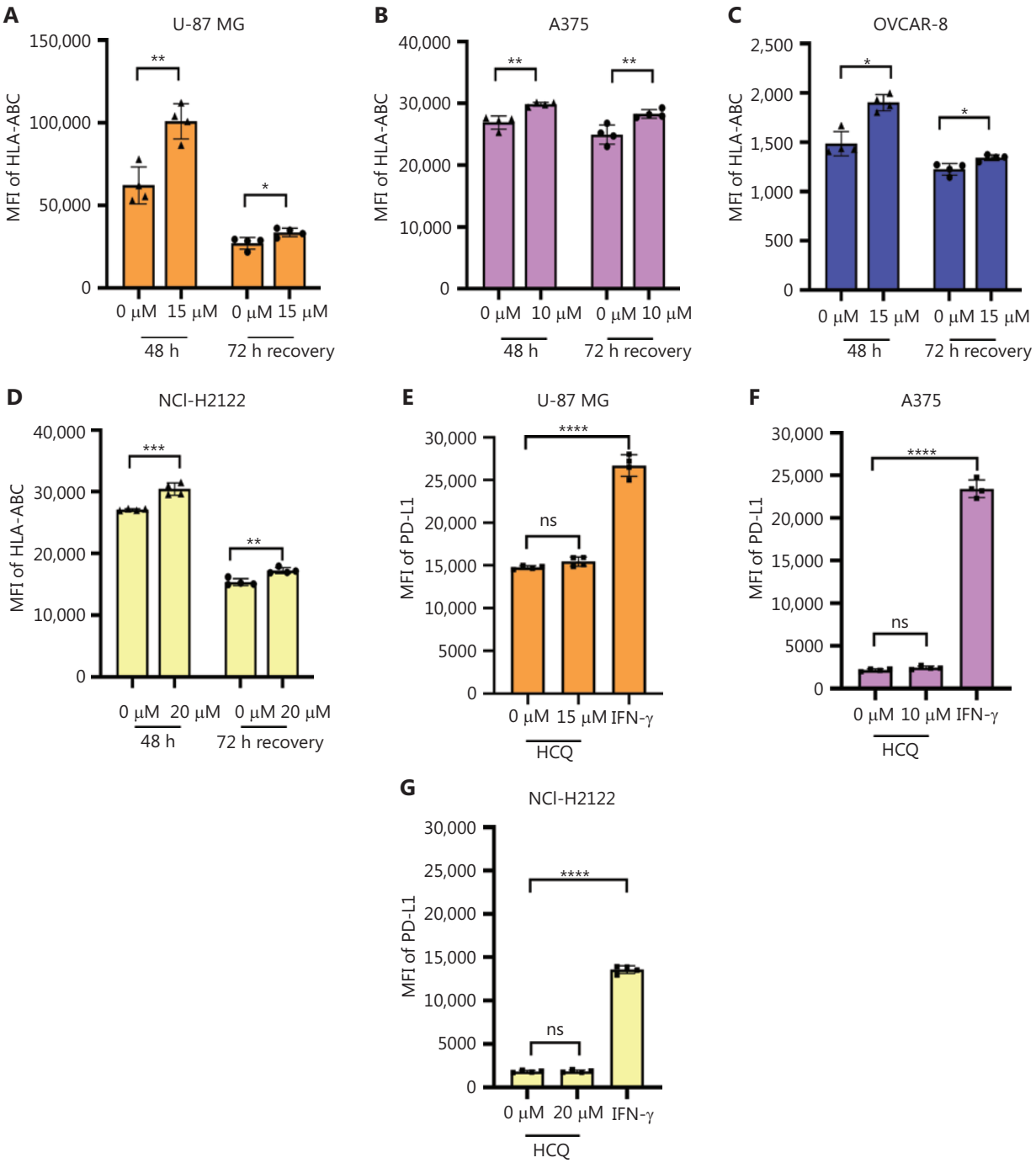


Figure 3 HCQ modulates MHC-I and PD-L1 expression in tumor cells. (A–D) Surface MHC-I (HLA-ABC) levels in U-87 MG, A-375, OVCAR-8, and NCI-H2122 cells after hydroxychloroquine (HCQ) treatment for 48 h and following a 72-h recovery period post-drug withdrawal (n = 4 per group). HCQ increased MHC-I expression, and partial recovery was observed after drug removal. (E–G) Programmed cell death ligand 1 (PD-L1) expression in U-87 MG, A375, and NCI-H2122 cells after 48-h exposure to HCQ or interferon-gamma (IFN-γ), compared with untreated controls (n = 4 each). IFN-γ strongly induced PD-L1, whereas HCQ exerted minimal effects. Mean fluorescence intensity (MFI) was measured with flow cytometry. Data are presented as mean ± SD. Two-group comparisons were analyzed with unpaired t-test or Mann–Whitney U-test. Three-group comparisons were analyzed with one-way analysis of variance (ANOVA) with Tukey's post-hoc test. ns, not significant; *P < 0.05; **P < 0.01; ***P < 0.001; and ****P < 0.0001.

higher body weights than observed in the TIL-only group (n = 7, P = 0.038) and control group (n = 5, P = 0.002); moreover, no significant difference was observed between the TIL-only and control groups (P = 0.478) (**Figure 4A**). At the endpoint, 2 mice in the TIL-only group succumbed to cachexia before sample collection and were therefore unavailable for endpoint tumor volume measurement and tumor weight–based analyses. Among evaluable animals, tumor growth was most suppressed in the combination group (n = 7), which showed significantly smaller tumor volumes than the control group (n = 5, P = 0.002). The TIL-only group had intermediate values that did not significantly differ with respect to the control group (n = 7 initially; n = 5 at the endpoint; P > 0.05) (**Figure 4C**). Furthermore, the combination group showed the lowest mean tumor weights and tumor-to-body weight ratios, although intergroup differences were not statistically significant (P > 0.05) (**Figure 4B, D**; n = 5 for TIL-only). The TGI rates were 34.95% in the combination group *vs.* 22.37% in the TIL-only group (**Table 1**). Tumor ulceration occurred in 3 mice each in the TIL-only and control groups, but was absent in the combination group. Overall, TIL monotherapy showed moderate antitumor activity with limited durability, whereas low-dose PD-1 blockade addition correlated with significantly improved weight maintenance, superior tumor growth control, and complete prevention of tumor ulceration in this model.

Discussion

Adoptive cell therapy with TILs is a promising strategy for treating solid tumors, but its broader clinical application is limited by multiple resistance mechanisms, including T-cell dysfunction and exhaustion, insufficient tumor recognition, antigen loss, and impaired T-cell trafficking[31-33]. Herein, we developed a novel TIL expansion platform to improve expansion consistency and generate functionally competent TILs across tumor types. A schematic overview of the optimized TIL therapy process is illustrated in **Figure 5**.

Traditional TIL expansion protocols commonly use high-dose IL-2 (> 3,000 IU/mL) and peripheral blood mononuclear cells as feeder cells to drive robust proliferation, and achieve approximately 1,000–5,000-fold expansion[10,34,35]. Because high-dose IL-2 may drive T-cell exhaustion, prior studies have suggested that low-dose IL-2 conditions might limit terminal effector differentiation and promote more functional, memory-like T cells[36-38]. Our feeder-free protocol with low-dose IL-2 (300–2,000 IU/mL) supported the generation of highly viable, phenotypically pure TILs from various tumor types. Single-cell and multi-omics studies have shown that tumor-specific TME variations shape T-cell composition and infiltration[39-41]. In our study, MM, CxCa, and CRC tumors, which are characterized by high immunogenicity and an inflamed TME[20], produced $CD8^+$-dominant TIL populations, and these are associated with enhanced antitumor efficacy[42-44]. In contrast, PC- and GC-derived TILs showed a wider range of $CD8^+$ fractions among $CD3^+$ TILs in this small cohort, in line with the immunosuppressive TMEs of these cancers, which are enriched in myeloid-derived suppressor cells and regulatory T cells[45,46]. Importantly, clinical studies have demonstrated that $CD4^+$ T cells also exert strong cytotoxic activity and mediate durable clinical remission[47,48]. Consistent with these findings, our IFN-γ-release assays revealed that TILs from PCs and GCs retained potent antitumor function despite variable $CD8^+$ frequencies across patients. In line with previous reports[49-51], most TILs exhibited a TEM phenotype after REP. Notably, our modified pre-REP incorporating IL-7 and IL-15 supported the expansion of TILs while maintaining central memory-associated phenotypic features. Previous studies using conventional REP have reported that central memory–associated markers (e.g., CCR7) are often present at low frequencies in expanded $CD3^+$ T cells[52]. Collectively, these findings suggested that our decreased IL-2, feeder-free protocol might effectively support the *in vitro* expansion of TILs while maintaining an effector phenotype with cytotoxic potential in different tumor types. The specific cell types involved and the therapeutic efficacy of this approach remain to be explored in future studies.

Impaired antigen presentation remains a key barrier to effective TIL therapy, and IFN-γ pretreatment of tumor cells has been used to enhance MHC-I expression, and $CD8^+$ T cell–mediated tumor recognition and lysis[53]. However, IFN-γ secreted by immune cells within the TME can induce PD-L1 expression on tumor cells *via* JAK1/JAK2/STAT1 pathway activation[54,55] and is associated with T-cell exhaustion and mutations in antigen presentation genes, thus leading to acquired resistance to immunotherapy[56]. HCQ, a derivative of the antimalarial drug chloroquine, inhibits autophagosome–lysosome fusion by elevating the lysosomal pH, thereby modulating autophagy[22,57,58]. Consequently, HCQ has demonstrated promising clinical antitumor activity[59,60]. By inhibiting autophagy, HCQ can restore MHC-I expression on cancer cell surfaces, and enhance antigen presentation and $CD8^+$ T cell–mediated antitumor responses[61,62]. This effect, reflected by increased membrane MHC-I levels, has been demonstrated in our previous work and other studies using established methods, such as analysis of autophagy-related proteins (e.g., LC3 and p62) and measurement of autophagic flux[63-66]. Beyond autophagy inhibition, HCQ increases tumor cell sensitivity by promoting the accumulation of reactive oxygen species, and subsequently inducing caspase-dependent apoptosis and inhibiting TLR signaling[65,67]. HCQ also repolarizes M2 tumor–associated macrophages to an M1-like phenotype, increases $CD8^+$ T–cell infiltration, and decreases immunosuppression in the TME[24], thereby enhancing TIL therapy efficacy and improving clinical outcomes. Our *in vitro* and PDX results suggested that HCQ increases MHC-I expression without affecting PD-L1 and exerts potential combinatorial effects with TIL therapy. However, the small sample size and

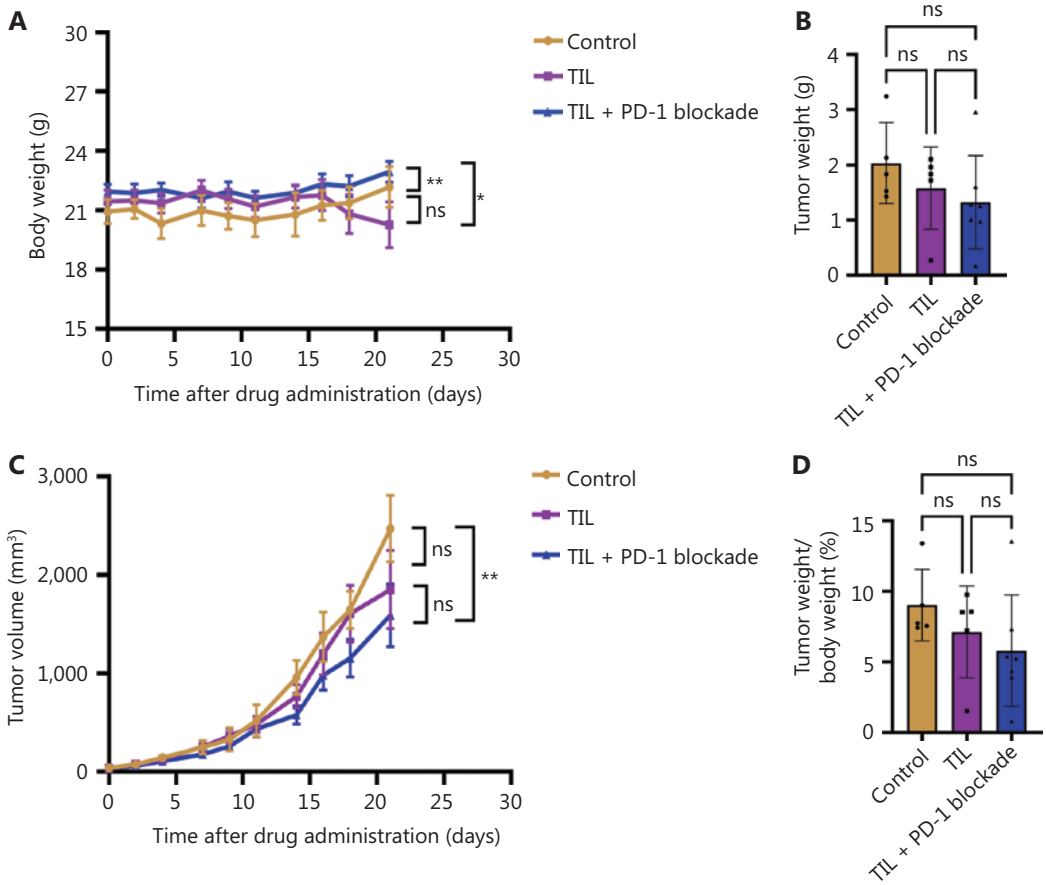


Figure 4 Antitumor activity of TIL combined with PD-1 blockade in colorectal cancer PDX mice. (A) Body weight changes in mice over the treatment course. The combination group (n = 7) maintained higher body weights than the TIL-only (n = 7, P = 0.038) and control (n = 5, P = 0.002) groups. (B) Isolated tumor weights at the experimental endpoint; two TIL-only mice were unavailable; therefore, n = 5 for the TIL-only group. Among evaluable mice, the combination group showed the lowest tumor weight (ns). (C) Tumor growth curves. Tumor volumes were significantly lower in the combination group (n = 7) than in the control group (n = 5, P = 0.002); the TIL-only group showed intermediate values (TIL-only: n = 7 initially, n = 5 at endpoint; ns). (D) Tumor weight–to–body weight ratio at endpoint; n = 5 for the TIL-only group. The combination group exhibited the lowest ratio (ns). Data represent mean ± SEM. Statistical significance was determined with one-way/two-way ANOVA with Tukey's post-hoc test (or Kruskal–Wallis with Dunn's post-hoc test, as appropriate). ns, not significant; *P < 0.05; **P < 0.01; ***P < 0.001; and ****P < 0.0001.

Table 1 Effects of TIL and PD-1 blockade in a colorectal cancer PDX model

Group	n	Tumor weight (g)	Tumor weight/body weight (%)	TGI (%)
Control	5	2.03 ± 0.33	9.03 ± 1.13	-
TIL therapy	5	1.58 ± 0.33	7.13 ± 1.45	22.37
TIL + PD-1 blockade	7	1.32 ± 0.32	5.80 ± 1.49	34.95

PD-1, programmed cell death protein 1; PDX, patient-derived xenograft; TGI, tumor growth inhibition; TIL, tumor-infiltrating lymphocyte. Data are presented as mean ± standard error of mean (SEM).

limited mechanistic data preclude definitive conclusions from being drawn and highlight the need for further investigation.

The PD-1/PD-L1 axis plays a central role in regulating T-cell function and shaping the TME, and its blockade has been shown in preclinical studies to restore T-cell activity and enhance the migration and function of transferred T cells at tumor sites[68-70]. Combining TIL therapy with PD-1 blockade has been explored as a strategy to improve the efficacy and durability of antitumor responses[71,72]. Pharmacodynamic studies have shown that low-dose PD-1 blockade can achieve

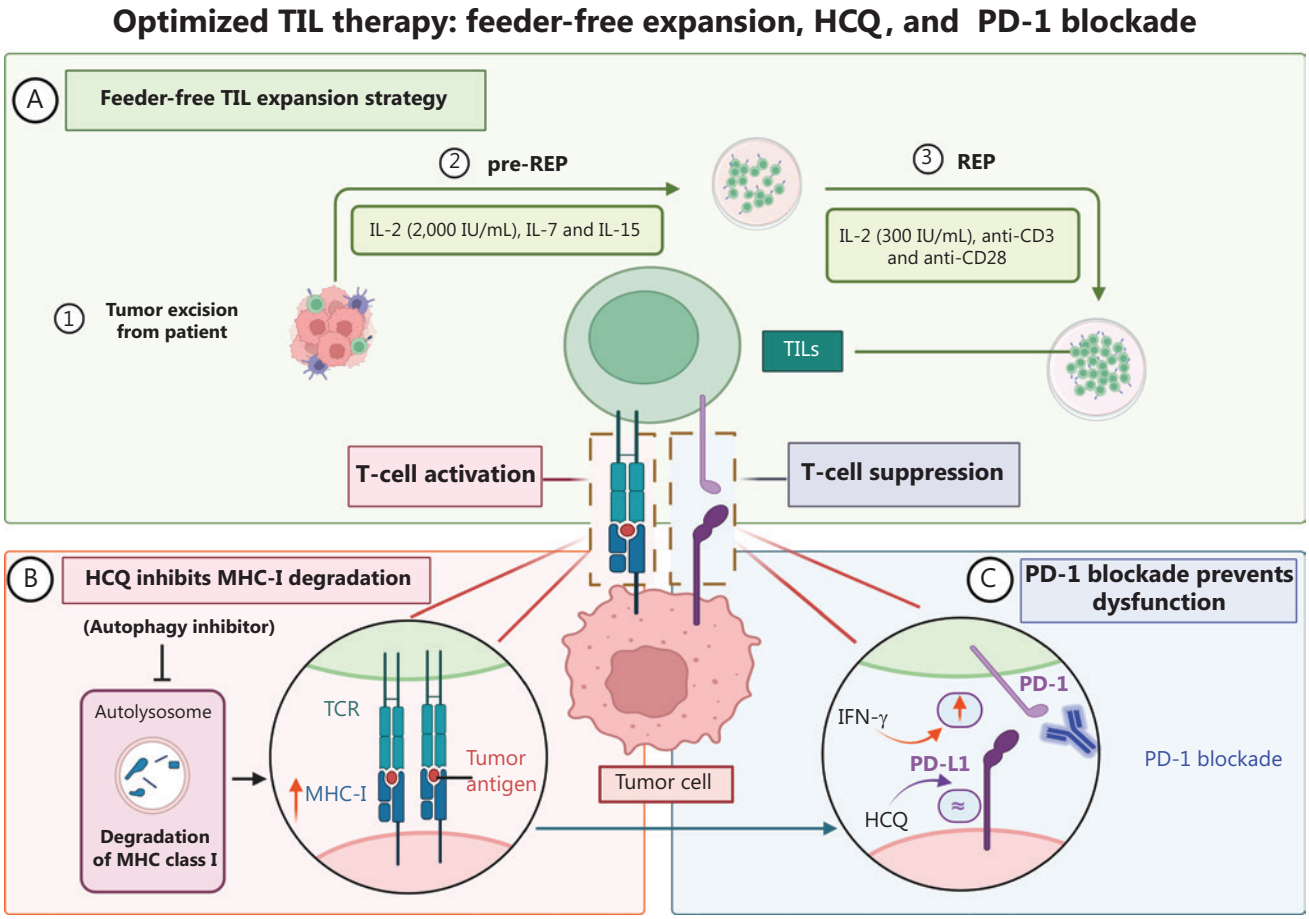


Figure 5 Mechanistic overview of optimized TIL therapy. (A) TILs were isolated from excised tumor tissues and expanded in a feeder-free culture system with low-dose IL-2 (2,000 IU/mL), IL-7, and IL-15 in the pre-REP phase, followed by low-dose IL-2 (300 IU/mL) with anti-CD3/CD28 stimulation in the REP phase. (B) HCQ, an autophagy inhibitor, increased MHC-I expression, potentially enhancing the antigen presentation to TCR and promoting T-cell activation. (C) PD-1 blockade prevented T-cell dysfunction, thus maintaining TIL cytotoxicity and tumor-killing ability. IFN-γ upregulated PD-L1 expression, and HCQ had no significant effect on PD-L1 levels. (Figure created in https://BioRender.com.) HCQ, hydroxychloroquine; IFN-γ, interferon-gamma; IL-15, interleukin-15; IL-2, interleukin-2; IL-7, interleukin-7; MHC-I, major histocompatibility complex class I; PD-1, programmed cell death protein 1; PD-L1, programmed death-ligand 1; pre-REP, pre-rapid expansion protocol; REP, rapid expansion protocol; TCR, T-cell receptor; TIL, tumor-infiltrating lymphocyte.

sufficient receptor occupancy (70.0%–75.0%) for T-cell activation, thus resulting in outcomes comparable to those achieved in standard dosing[26,73,74]. To sustain TIL persistence while avoiding the toxicity of high-dose IL-2, we evaluated low-dose PD-1 blockade as an alternative supportive approach. In a CRC PDX model, administration of low-dose PD-1 blockade (2 mg/kg) in combination with TIL produced the most pronounced tumor control, although this finding was limited by the use of a single model. This IL-2-independent strategy has also been examined in CxCa PDX model by other groups and subsequently tested in a clinical trial in patients with advanced gynecologic cancers, using oral HCQ preconditioning and low-dose PD-1 blockade at infusion and thereafter without intravenous IL-2; early results showed favorable safety and preliminary antitumor activity[29,30].

Despite these promising outcomes, this study has several limitations. The small sample size and use of a single CRC PDX model limit the generalizability of the findings. In addition, the *in vitro* TCR-T model used a single tumor antigen (NY-ESO-1), which might not reflect the broader antigenic heterogeneity of TILs. Moreover, because systematic and mechanistic investigations of the combined effects of HCQ and PD-1 blockade with TIL therapy were limited in our study, their precise roles in modulating TIL function and the TME remain underexplored; no post-infusion high-dose IL-2 support arm was included. Future studies should increase the sample size and validate this strategy in additional tumor models beyond CRC, to address tumor-specific differences in TIL phenotypes and functions. In addition, integrated multi-omics approaches are needed to elucidate the mechanisms underlying the potential synergy of

TIL therapy with HCQ and PD-1 blockade, and to identify predictive biomarkers for clinical translation.

Conclusions

We developed a feeder-free, low-dose IL-2 TIL expansion system that supports TIL therapy without post-infusion IL-2 administration in this study. Low-dose PD-1 blockade enhanced antitumor efficacy *in vivo*, whereas HCQ increased MHC-I expression and early T-cell cytotoxicity *in vitro* but showed limited *in vivo* efficacy, potentially because of the small sample sizes. Future studies should include expanded *in vivo* validation, and further investigation of the mechanisms underlying TIL persistence and TME modulation.

Acknowledgements

We acknowledge Prof. Xiao Zhao for administrative assistance during the ethics approval process. We also sincerely thank Dr. Feng Yin from Shanghai Juncell Biotechnology Co., Ltd. for project coordination and Nanchang Leyou Biotechnology Co., Ltd. for technical support in conducting the animal experiments.

Grant support

This study was supported by the Science and Technology Innovation Action Plan of the Science and Technology Commission of Shanghai Municipality (STCSM) (Grant No. 22XD1432200).

Conflict of interest statement

The authors declare the following competing interests: Man Zhang, Xingming Ma, Zhou He, Wenjia Zhuang, and Huajun Jin are employees of Shanghai Juncell Biotechnology Co., Ltd. All other authors declare no competing interests.

Author contributions

Conceptualization and study design: Huajun Jin, Jianming Xu.
Methodology and investigation: Ying Zhang, Sicheng Du, Rongrui Liu, Chuanhua Zhao, Juan Li, Sisi Ye, Man Zhang, Xingming Ma, Zhou He, Wenjia Zhuang.
Data curation: Ying Zhang, Man Zhang, Xingming Ma, Zhou He, Wenjia Zhuang.
Technical support: Huajun Jin.
Project administration: Huajun Jin, Jianming Xu.
Funding acquisition: Huajun Jin.
Supervision: Huajun Jin, Jianming Xu.
Data analysis: Ying Zhang and Wenjia Zhuang.
Writing—original draft: Ying Zhang and Wenjia Zhuang.
Writing—review & editing: All authors.

Data availability statement

The data generated in this study are available upon request from the corresponding author.

References

1. Albarrán V, San Román M, Pozas J, Chamorro J, Rosero DI, Guerrero P, et al. Adoptive T cell therapy for solid tumors: current landscape and future challenges. Front Immunol. 2024; 15: 1352805.
2. Wang S, Sun J, Chen K, Ma P, Lei Q, Xing S, et al. Perspectives of tumor-infiltrating lymphocyte treatment in solid tumors. BMC Med. 2021; 19: 140.
3. Julve M, Lythgoe MP, Larkin J, Furness AJS. Lifileucel: the first cellular therapy approved for solid tumours. Trends Cancer. 2024; 10: 475-7.
4. Dudley ME, Wunderlich JR, Shelton TE, Even J, Rosenberg SA. Generation of tumor-infiltrating lymphocyte cultures for use in adoptive transfer therapy for melanoma patients. J Immunother. 2003; 26: 332-42.
5. Tran KQ, Zhou J, Durflinger KH, Langhan MM, Shelton TE, Wunderlich JR, et al. Minimally cultured tumor-infiltrating lymphocytes display optimal characteristics for adoptive cell therapy. J Immunother. 2008; 31: 742-51.
6. Gattinoni L, Klebanoff CA, Palmer DC, Wrzesinski C, Kerstann K, Yu Z, et al. Acquisition of full effector function in vitro paradoxically impairs the in vivo antitumor efficacy of adoptively transferred $CD8^+$ T cells. J Clin Invest. 2005; 115: 1616-26.
7. Rosenberg SA. IL-2: the first effective immunotherapy for human cancer. J Immunol. 2014; 192: 5451-8.
8. Chesney J, Lewis KD, Kluger H, Hamid O, Whitman E, Thomas S, et al. Efficacy and safety of lifileucel, a one-time autologous tumor-infiltrating lymphocyte (TIL) cell therapy, in patients with advanced melanoma after progression on immune checkpoint inhibitors and targeted therapies: pooled analysis of consecutive cohorts of the C-144-01 study. J Immunother Cancer. 2022; 10: e005755.
9. Dudley ME, Gross CA, Langhan MM, Garcia MR, Sherry RM, Yang JC, et al. $CD8^+$ enriched "young" tumor infiltrating lymphocytes can mediate regression of metastatic melanoma. Clin Cancer Res. 2010; 16: 6122-31.
10. Itzhaki O, Hovav E, Ziporen Y, Levy D, Kubi A, Zikich D, et al. Establishment and large-scale expansion of minimally cultured "young" tumor infiltrating lymphocytes for adoptive transfer therapy. J Immunother. 2011; 34: 212-20.

11. Boyman O, Sprent J. The role of interleukin-2 during homeostasis and activation of the immune system. Nat Rev Immunol. 2012; 12: 180-90.
12. Liu Y, Zhou N, Zhou L, Wang J, Zhou Y, Zhang T, et al. IL-2 regulates tumor-reactive $CD8^+$ T cell exhaustion by activating the aryl hydrocarbon receptor. Nat Immunol. 2021; 22: 358-69.
13. Le HK, Graham L, Miller CHT, Kmieciak M, Manjili MH, Bear HD. Incubation of antigen-sensitized T lymphocytes activated with bryostatin 1 + ionomycin in IL-7 + IL-15 increases yield of cells capable of inducing regression of melanoma metastases compared to culture in IL-2. Cancer Immunol Immunother. 2009; 58: 1565-76.
14. Cha E, Graham L, Manjili MH, Bear HD. IL-7 + IL-15 are superior to IL-2 for the ex vivo expansion of 4T1 mammary carcinoma-specific T cells with greater efficacy against tumors in vivo. Breast Cancer Res Treat. 2010; 122: 359-69.
15. Cieri N, Camisa B, Cocchiarella F, Forcato M, Oliveira G, Provasi E, et al. IL-7 and IL-15 instruct the generation of human memory stem T cells from naive precursors. Blood. 2013; 121: 573-84.
16. Li Y, Liu S, Hernandez J, Vence L, Hwu P, Radvanyi L. MART-1-specific melanoma tumor-infiltrating lymphocytes maintaining CD28 expression have improved survival and expansion capability following antigenic restimulation in vitro. J Immunol. 2010; 184: 452-65.
17. Zhou J, Shen X, Huang J, Hodes RJ, Rosenberg SA, Robbins PF. Telomere length of transferred lymphocytes correlates with in vivo persistence and tumor regression in melanoma patients receiving cell transfer therapy. J Immunol. 2005; 175: 7046-52.
18. Radvanyi LG, Shi Y, Vaziri H, Sharma A, Dhala R, Mills GB, et al. CD28 costimulation inhibits TCR-induced apoptosis during a primary T cell response. J Immunol. 1996; 156: 1788-98.
19. Nijhuis EW, vd Wiel-van Kemenade E, Figdor CG, van Lier RA. Activation and expansion of tumour-infiltrating lymphocytes by anti-CD3 and anti-CD28 monoclonal antibodies. Cancer Immunol Immunother. 1990; 32: 245-50.
20. Fridman WH, Pagès F, Sautès-Fridman C, Galon J. The immune contexture in human tumours: impact on clinical outcome. Nat Rev Cancer. 2012; 12: 298-306.
21. Mendez R, Aptsiauri N, Del Campo A, Maleno I, Cabrera T, Ruiz-Cabello F, et al. HLA and melanoma: multiple alterations in HLA class I and II expression in human melanoma cell lines from ESTDAB cell bank. Cancer Immunol Immunother. 2009; 58: 1507-15.
22. Yamamoto K, Venida A, Yano J, Biancur DE, Kakiuchi M, Gupta S, et al. Autophagy promotes immune evasion of pancreatic cancer by degrading MHC-I. Nature. 2020; 581: 100-5.
23. Chude CI, Amaravadi RK. Targeting autophagy in cancer: update on clinical trials and novel inhibitors. Int J Mol Sci. 2017; 18: 1279.
24. Li Y, Cao F, Li M, Li P, Yu Y, Xiang L, et al. Hydroxychloroquine induced lung cancer suppression by enhancing chemo-sensitization and promoting the transition of M2-TAMs to M1-like macrophages. J Exp Clin Cancer Res. 2018; 37: 259.
25. Wang J, Fei K, Jing H, Wu Z, Wu W, Zhou S, et al. Durable blockade of PD-1 signaling links preclinical efficacy of sintilimab to its clinical benefit. MAbs. 2019; 11: 1443-51.
26. Brahmer JR, Drake CG, Wollner I, Powderly JD, Picus J, Sharfman WH, et al. Phase I study of single-agent anti-programmed death-1 (MDX-1106) in refractory solid tumors: safety, clinical activity, pharmacodynamics, and immunologic correlates. J Clin Oncol. 2010; 28: 3167-75.
27. Zhang L, Mai W, Jiang W, Geng Q. Sintilimab: a promising anti-tumor PD-1 antibody. Front Oncol. 2020; 10: 594558.
28. Hoy SM. Sintilimab: first global approval. Drugs. 2019; 79: 341-6.
29. Guo J, Luo N, Ai G, Yang W, Zhu J, Li C, et al. Eradicating tumor in a recurrent cervical cancer patient with autologous tumor-infiltrating lymphocytes and a modified lymphodepleting regimen. J Immunother Cancer. 2022; 10: e003887.
30. Guo J, Wang C, Luo N, Wu Y, Huang W, Zhu J, et al. IL-2-free tumor-infiltrating lymphocyte therapy with PD-1 blockade demonstrates potent efficacy in advanced gynecologic cancer. BMC Med. 2024; 22: 207.
31. Dafni U, Michielin O, Lluesma SM, Tsourti Z, Polydoropoulou V, Karlis D, et al. Efficacy of adoptive therapy with tumor-infiltrating lymphocytes and recombinant interleukin-2 in advanced cutaneous melanoma: a systematic review and meta-analysis. Ann Oncol. 2019; 30: 1902-13.
32. Betof Warner A, Corrie PG, Hamid O. Tumor-infiltrating lymphocyte therapy in melanoma: facts to the future. Clin Cancer Res. 2023; 29: 1835-54.
33. Qin SS, Melucci AD, Chacon AC, Prieto PA. Adoptive T cell therapy for solid tumors: pathway to personalized standard of care. Cells. 2021; 10: 808.
34. Besser MJ, Shapira-Frommer R, Treves AJ, Zippel D, Itzhaki O, Schallmach E, et al. Minimally cultured or selected autologous tumor-infiltrating lymphocytes after a lympho-depleting chemotherapy regimen in metastatic melanoma patients. J Immunother. 2009; 32: 415-23.
35. Andersen R, Donia M, Ellebaek E, Borch TH, Kongsted P, Iversen TZ, et al. Long-lasting complete responses in patients with metastatic melanoma after adoptive cell therapy with tumor-infiltrating lymphocytes and an attenuated IL2 regimen. Clin Cancer Res. 2016; 22: 3734-45.
36. Besser MJ, Schallmach E, Oved K, Treves AJ, Markel G, Reiter Y, et al. Modifying interleukin-2 concentrations during culture improves function of T cells for adoptive immunotherapy. Cytotherapy. 2009; 11: 206-17.
37. Kaartinen T, Luostarinen A, Maliniemi P, Keto J, Arvas M, Belt H, et al. Low interleukin-2 concentration favors generation of early memory T cells over effector phenotypes during chimeric antigen receptor T-cell expansion. Cytotherapy. 2017; 19: 689-702.
38. Kongkaew T, Thaiwong R, Tudsamran S, Sae-Jung T, Sengprasert P, Vasuratna A, et al. TIL expansion with high dose IL-2 or low dose IL-2 with anti-CD3/anti-CD28 stimulation provides different quality of TIL-expanded T cell clones. J Immunol Methods. 2022; 503: 113229.

39. Zheng L, Qin S, Si W, Wang A, Xing B, Gao R, et al. Pan-cancer single-cell landscape of tumor-infiltrating T cells. Science. 2021; 374: abe6474.
40. Quek C, Pratapa A, Bai X, Al-Eryani G, Pires da Silva I, Mayer A, et al. Single-cell spatial multiomics reveals tumor microenvironment vulnerabilities in cancer resistance to immunotherapy. Cell Rep. 2024; 43: 114392.
41. Yang W, Liu S, Mao M, Gong Y, Li X, Lei T, et al. T-cell infiltration and its regulatory mechanisms in cancers: insights at single-cell resolution. J Exp Clin Cancer Res. 2024; 43: 38.
42. Krishna S, Lowery FJ, Copeland AR, Bahadiroglu E, Mukherjee R, Jia L, et al. Stem-like CD8 T cells mediate response of adoptive cell immunotherapy against human cancer. Science. 2020; 370: 1328-34.
43. Besser MJ, Shapira-Frommer R, Itzhaki O, Treves AJ, Zippel DB, Levy D, et al. Adoptive transfer of tumor-infiltrating lymphocytes in patients with metastatic melanoma: intent-to-treat analysis and efficacy after failure to prior immunotherapies. Clin Cancer Res. 2013; 19: 4792-800.
44. Djenidi F, Adam J, Goubar A, Durgeau A, Meurice G, de Montpréville V, et al. $CD8^+CD103^+$ tumor-infiltrating lymphocytes are tumor-specific tissue-resident memory T cells and a prognostic factor for survival in lung cancer patients. J Immunol. 2015; 194: 3475-86.
45. Wang Y, Ding N, Qi L, Chen W, Wu P. Immunopharmacology of gastric cancer-deciphering immune cell subset responses and nanoparticle-mediated targeting. Front Pharmacol. 2025; 16: 1611234.
46. Pan D, Li X, Qiao X, Wang Q. Immunosuppressive tumor microenvironment in pancreatic cancer: mechanisms and therapeutic targets. Front Immunol. 2025; 16: 1582305.
47. Tran E, Turcotte S, Gros A, Robbins PF, Lu YC, Dudley ME, et al. Cancer immunotherapy based on mutation-specific $CD4^+$ T cells in a patient with epithelial cancer. Science. 2014; 344: 641-5.
48. Hunder NN, Wallen H, Cao J, Hendricks DW, Reilly JZ, Rodmyre R, et al. Treatment of metastatic melanoma with autologous $CD4^+$ T cells against NY-ESO-1. N Engl J Med. 2008; 358: 2698-703.
49. Amaria R, Knisely A, Vining D, Kopetz S, Overman MJ, Javle M, et al. Efficacy and safety of autologous tumor-infiltrating lymphocytes in recurrent or refractory ovarian cancer, colorectal cancer, and pancreatic ductal adenocarcinoma. J Immunother Cancer. 2024; 12: e006822.
50. Chiffelle J, Barras D, Pétremand R, Orcurto A, Bobisse S, Arnaud M, et al. Tumor-reactive T cell clonotype dynamics underlying clinical response to TIL therapy in melanoma. Immunity. 2024; 57: 2466-82.e12.
51. Borch TH, Harbst K, Rana AH, Andersen R, Martinenaite E, Kongsted P, et al. Clinical efficacy of T-cell therapy after short-term BRAF-inhibitor priming in patients with checkpoint inhibitor-resistant metastatic melanoma. J Immunother Cancer. 2021; 9: e002703.
52. Kverneland AH, Chamberlain CA, Borch TH, Nielsen M, Mørk SK, Kjeldsen JW, et al. Adoptive cell therapy with tumor-infiltrating lymphocytes supported by checkpoint inhibition across multiple solid cancer types. J Immunother Cancer. 2021; 9: e003499.
53. Donia M, Hansen M, Sendrup SL, Iversen TZ, Ellebæk E, Andersen MH, et al. Methods to improve adoptive T-cell therapy for melanoma: IFN-γ enhances anticancer responses of cell products for infusion. J Invest Dermatol. 2013; 133: 545-52.
54. Knopf P, Stowbur D, Hoffmann SHL, Hermann N, Maurer A, Bucher V, et al. Acidosis-mediated increase in IFN-γ-induced PD-L1 expression on cancer cells as an immune escape mechanism in solid tumors. Mol Cancer. 2023; 22: 207.
55. Garcia-Diaz A, Shin DS, Moreno BH, Saco J, Escuin-Ordinas H, Rodriguez GA, et al. Interferon receptor signaling pathways regulating PD-L1 and PD-L2 expression. Cell Reports. 2017; 19: 1189-201.
56. Memon D, Schoenfeld AJ, Ye D, Fromm G, Rizvi H, Zhang X, et al. Clinical and molecular features of acquired resistance to immunotherapy in non-small cell lung cancer. Cancer Cell. 2024; 42: 209-24.e9.
57. Zeh HJ, Bahary N, Boone BA, Singhi AD, Miller-Ocuin JL, Normolle DP, et al. A randomized phase II preoperative study of autophagy inhibition with high-dose hydroxychloroquine and gemcitabine/nab-paclitaxel in pancreatic cancer patients. Clin Cancer Res. 2020; 26: 3126-34.
58. Kinsey CG, Camolotto SA, Boespflug AM, Guillen KP, Foth M, Truong A, et al. Protective autophagy elicited by RAF→MEK→ERK inhibition suggests a treatment strategy for RAS-driven cancers. Nat Med. 2019; 25: 620-7.
59. Gong C, Lin Q, Qin T, Zeng Y, Xu F, Yang Y, et al. Targeting autophagy plus high-dose CDK4/6 inhibitors in advanced HR+HER2− breast cancer: a phase 1b/2 trial. Med. 2025; 6: 100559.
60. AlMasri SS, Zenati MS, Desilva A, Nassour I, Boone BA, Singhi AD, et al. Encouraging long-term survival following autophagy inhibition using neoadjuvant hydroxychloroquine and gemcitabine for high-risk patients with resectable pancreatic carcinoma. Cancer Med. 2021; 10: 7233-41.
61. Agalakova NI. Chloroquine and chemotherapeutic compounds in experimental cancer treatment. Int J Mol Sci. 2024; 25: 945.
62. Liu J, Liu X, Han Y, Zhang J, Liu D, Ma G, et al. Nanovaccine incorporated with hydroxychloroquine enhances antigen cross-presentation and promotes antitumor immune responses. ACS Appl Mater Interfaces. 2018; 10: 30983-93.
63. Lin YC, Lin JF, Wen SI, Yang SC, Tsai TF, Chen HE, et al. Chloroquine and hydroxychloroquine inhibit bladder cancer cell growth by targeting basal autophagy and enhancing apoptosis. Kaohsiung J Med Sci. 2017; 33: 215-23.
64. Zhang H, Wang Y, Zhu L, Qi Z, Cao K, Chang J, et al. A "bulldozer" driven by anoxic bacteria for pancreatic cancer chemo-immunotherapy. J Control Release. 2023; 360: 660-71.
65. Peng X, Zhang S, Jiao W, Zhong Z, Yang Y, Claret FX, et al. Hydroxychloroquine synergizes with the PI3K inhibitor BKM120 to exhibit antitumor efficacy independent of autophagy. J Exp Clin Cancer Res. 2021; 40: 374.
66. Zhang M, Huang C, Ma X, Zhuang W, Jin H. Hydroxychloroquine increases the tumor killing efficiency via elevating the membrane MHC-I protein levels of tumor cells. Cancer Res. 2025; 85(Suppl): Abstract 5827.

67. Ferreira PMP, de Sousa RWR, de Ferreira JRO, Militão GCG, Bezerra DP. Chloroquine and hydroxychloroquine in antitumor therapies based on autophagy-related mechanisms. Pharmacol Res. 2021; 168: 105582.
68. Blank C, Brown I, Peterson AC, Spiotto M, Iwai Y, Honjo T, et al. PD-L1/B7H-1 inhibits the effector phase of tumor rejection by T cell receptor (TCR) transgenic CD8$^+$ T cells. Cancer Res. 2004; 64: 1140-5.
69. Peng W, Liu C, Xu C, Lou Y, Chen J, Yang Y, et al. PD-1 blockade enhances T-cell migration to tumors by elevating IFN-γ inducible chemokines. Cancer Res. 2012; 72: 5209-18.
70. Fernandez-Poma SM, Salas-Benito D, Lozano T, Casares N, Riezu-Boj JI, Mancheño U, et al. Expansion of tumor-infiltrating CD8$^+$ T cells expressing PD-1 improves the efficacy of adoptive T-cell therapy. Cancer Res. 2017; 77: 3672-84.
71. Davies JS, Karimipour F, Zhang L, Nagarsheth N, Norberg S, Serna C, et al. Non-synergy of PD-1 blockade with T-cell therapy in solid tumors. J Immunother Cancer. 2022; 10: e004906.
72. Hall MS, Mullinax JE, Cox CA, Hall AM, Beatty MS, Blauvelt J, et al. Combination Nivolumab, CD137 agonism, and adoptive cell therapy with tumor-infiltrating lymphocytes for patients with metastatic melanoma. Clin Cancer Res. 2022; 28(24): 5317-29.
73. Agrawal S, Feng Y, Roy A, Kollia G, Lestini B. Nivolumab dose selection: challenges, opportunities, and lessons learned for cancer immunotherapy. J Immunother Cancer. 2016; 4: 72.
74. Jiménez-Labaig P, Mohamed F, Tan NJI, Sanna I, El Bairi K, Khan SZ, et al. Expanding access to cancer immunotherapy: a systematic review of low-dose PD-(L)1 inhibitor strategies. Eur J Cancer. 2025; 225: 115564.

Cite this article as: Zhang Y, Du S, Liu R, Zhao C, Li J, Ye S, et al. Expansion of IL-2-independent tumor-infiltrating lymphocytes through a feeder-free process: a preclinical study for solid tumors. Cancer Biol Med. 2026; 23: 910-924. doi: 10.20892/j.issn.2095-3941.2025.0441